Transient State Kinetic Studies of the MutT-Catalyzed Nucleoside Triphosphate Pyrophosphohydrolase Reaction†

Zuyong Xia, Hugo F. Azurmendi, and Albert S. Mildvan*

Department of Biological Chemistry, The Johns Hopkins School of Medicine, 725 North Wolfe Street, Baltimore, Maryland 21205-2185

Received July 13, 2005; Revised Manuscript Received September 20, 2005

ABSTRACT: The MutT pyrophosphohydrolase, in the presence of Mg^{2+}, catalyzes the hydrolysis of nucleoside triphosphates by nucleophilic substitution at Pβ, to yield the nucleotide and PP_i. The best substrate for MutT is the mutagenic 8-oxo-dGTP, on the basis of its K_m being 540-fold lower than that of dGTP. Product inhibition studies have led to a proposed uni-bi-iso kinetic mechanism, in which PP_i dissociates first from the enzyme−product complex (k_3), followed by NMP (k_4), leaving a product-binding form of the enzyme (F) which converts to the substrate-binding form (E) in a partially rate-limiting step (k_5) [Saraswat, V., et al. (2002) *Biochemistry 41*, 15566−15577]. Single- and multiple-turnover kinetic studies of the hydrolysis of dGTP and 8-oxo-dGTP and global fitting of the data to this mechanism have yielded all of the nine rate constants. Consistent with an "iso" mechanism, single-turnover studies with dGTP and 8-oxo-dGTP hydrolysis showed slow apparent second-order rate constants for substrate binding similar to their k_{cat}/K_m values, but well below the diffusion limit ($\sim 10^9$ M^{-1} s^{-1}): $k_{on}^{app} = 7.2 \times 10^4$ M^{-1} s^{-1} for dGTP and $k_{on}^{app} = 2.8 \times 10^7$ M^{-1} s^{-1} for 8-oxo-dGTP. These low k_{on}^{app} values are fitted by assuming a slow iso step ($k_5 = 12.1$ s^{-1}) followed by fast rate constants for substrate binding: $k_1 = 1.9 \times 10^6$ M^{-1} s^{-1} for dGTP and $k_1 = 0.75 \times 10^9$ M^{-1} s^{-1} for 8-oxo-dGTP (the latter near the diffusion limit). With dGTP as the substrate, replacing Mg^{2+} with Mn^{2+} does not change k_1, consistent with the formation of a second-sphere MutT−M^{2+}−(H_2O)−dGTP complex, but slows the iso step (k_5) 5.8-fold, and its reverse (k_{-5}) 25-fold, suggesting that the iso step involves a change in metal coordination, likely the dissociation of Glu-53 from the enzyme-bound metal so that it can function as the general base. Multiple-turnover studies with dGTP and 8-oxo-dGTP show bursts of product formation, indicating partially rate-limiting steps following the chemical step (k_2). With dGTP, the slow steps are the chemical step ($k_2 = 10.7$ s^{-1}) and the iso step ($k_5 = 12.1$ s^{-1}). With 8-oxo-dGTP, the slow steps are the release of the 8-oxo-dGMP product ($k_4 = 3.9$ s^{-1}) and the iso step ($k_5 = 12.1$ s^{-1}), while the chemical step is fast ($k_2 = 32.3$ s^{-1}). The transient kinetic studies are generally consistent with the steady state k_{cat} and K_m values. Comparison of rate constants and free energy diagrams indicate that 8-oxo-dGTP, at low concentrations, is a better substrate than dGTP because it binds to MutT 395-fold faster, dissociates 46-fold slower, and has a 3.0-fold faster chemical step. The true dissociation constants (K_D) of the substrates from the E-form of MutT, which can now be obtained from k_{-1}/k_1, are 3.5 nM for 8-oxo-dGTP and 62 μM for dGTP, indicating that 8-oxo-dGTP binds 1.8×10^4-fold tighter than dGTP, corresponding to a 5.8 kcal/mol lower free energy of binding.

The MutT pyrophosphohydrolase from *Escherichia coli*, a monomeric enzyme containing 129 residues, is a prototypical Nudix hydrolase (*1*) that catalyzes the hydrolysis of nucleoside and deoxynucleoside triphosphates (NTP) by nucleophilic substitution at Pβ to yield the nucleotide (NMP) and inorganic pyrophosphate (PP_i) (*2*).

$$NTP + H_2O \rightarrow NMP + PP_i + H^+ \qquad (1)$$

The proposed biological role of MutT is the removal of damaged and mutagenic nucleotides, such as 8-oxo-dGTP (*3*), which can be misincorporated into DNA opposite template dA during DNA replication (*4*). Genetic inactivation of this enzyme or its homologue results in a 10^4-fold increase in AT → CG transversions in *E. coli* (*5*, *6*), and in an increased incidence of tumors in mice (*7*). While the in vivo substrate of MutT is unclear (*8*), the mutagenic nucleotide, 8-oxo-dGTP, is by far the best in vitro substrate, on the basis of its low K_m (*3*).

Structures and mechanisms of Nudix hydrolases have been reviewed (*9*, *10*). The solution structure (*11*−*13*) and chemical mechanism of the MutT enzyme have been extensively studied (*2*, *14*−*17*). The enzyme from *E. coli* requires two divalent cations for activity, one coordinated directly to the protein and the other coordinated to the β- and γ-phosphoryl groups of the NTP substrate (*14*). On the

† This research was supported by National Institutes of Health Grant DK28616 (to A.S.M.).

* To whom correspondence should be addressed. Phone: (410) 955-2038. E-mail: mildvan@jhmi.edu. Fax: (410) 955-5759.

10.1021/bi0513599 CCC: $30.25
Published on Web 10/26/2005

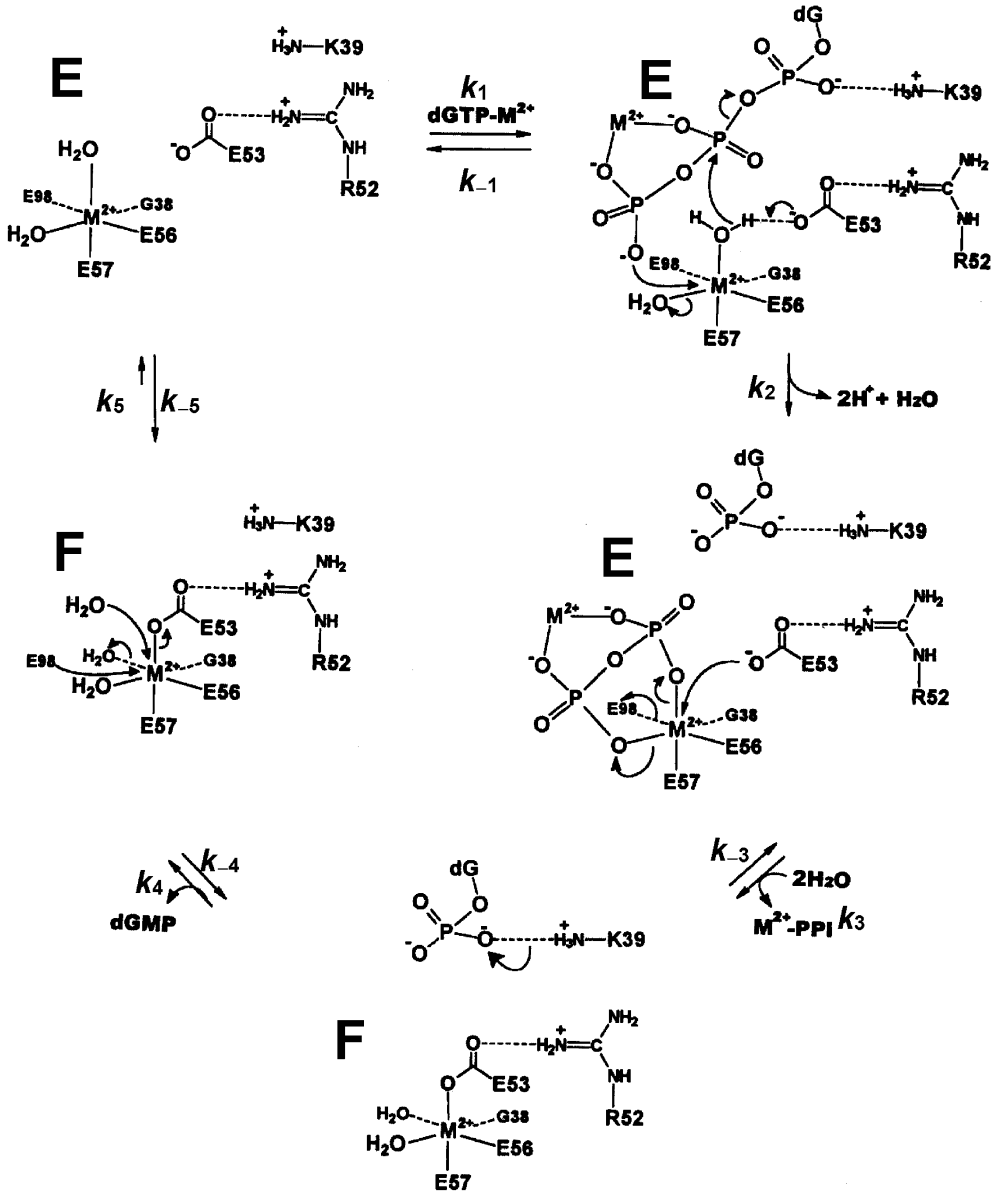

FIGURE 1: Proposed iso mechanism of the MutT reaction based on product inhibition (*17*), structural (*12*), and mutagenesis studies (*15*, *16*). E and F represent the enzyme conformations which bind the NTP substrate and the NMP product, respectively.

Scheme 1

$$E + NTP \underset{k_{-1}}{\overset{k_1}{\rightleftharpoons}} E{\bullet}NTP \xrightarrow{k_2} E{\bullet}NMP{\bullet}PP_i \underset{k_{-3}}{\overset{k_3,\ PP_i}{\rightleftharpoons}} F{\bullet}NMP \underset{k_{-4}}{\overset{k_4,\ NMP}{\rightleftharpoons}} F \underset{k_{-5}}{\overset{k_5}{\rightleftharpoons}} E$$

basis of the locations of the required divalent cations, and measured intersubstrate distances, an associative nucleophilic displacement at Pβ of the NTP by an activated water nucleophile was proposed, with stabilization of the leaving NMP by Lys-39 (Figure 1) (*12*). The effects of site specific mutations of active site residues on k_{cat} and K_m of the substrates dGTP and 8-oxo-dGTP, and on K_D values of the enzyme-bound metal activator and the dGMP and 8-oxo-dGMP products, were consistent with the chemical mechanism of Figure 1 (*15*, *16*).

An "iso" kinetic mechanism for MutT (Scheme 1 and Figure 1) was proposed on the basis of product inhibition studies of dGTP hydrolysis, which showed uncompetitive inhibition by $M^{2+}PP_i$ and *noncompetitive* rather than *competitive* inhibition by dGMP (*17*).

This kinetic mechanism includes an irreversible step, the hydrolysis of dGTP (k_2), followed by the ordered release of products, with $M^{2+}PP_i$ preceding dGMP. The intercept effect in the inhibition by NMP required that this product bind to a different form of the enzyme (F) than the form which binds substrate (E) (*17*). In the partially rate-limiting iso step (k_5), this altered form of the enzyme slowly reverts to the form that binds substrate (*17*−*21*).

In this paper, we have sought independent and more direct evidence for the iso kinetic mechanism of Figure 1 by transient state kinetic and viscosity studies of the MutT reaction. Chemical-quench-flow techniques (*22*) have been used to measure the rate constants of all of the steps in the kinetic mechanism, including NTP binding, NTP hydrolysis, product release, and enzyme isomerization, using dGTP and 8-oxo-dGTP as substrates. The transient kinetic approach has also provided insight into the chemical nature of the iso step, and a detailed explanation of the preferred hydrolysis of 8-oxo-dGTP, which was previously based solely on steady state k_{cat} and K_m values (*3*, *16*).

EXPERIMENTAL PROCEDURES

Materials. The construction of the plasmid pETMutT, containing the mutT gene under control of the T7 promoter (pET system, Novagen Inc., Madison, WI), has been described previously (*23*). Isopropyl β-D-thiogalactoside was from Roche (Indianapolis, IN). Tryptone and yeast extract were obtained from Difco (Detroit, MI). Ammonium sulfate, ampicillin, 2′-deoxyguanosine 5′-monophosphate, 2′-deoxycytidine 5′-monophosphate, 2′-deoxyguanosine 5′-diphosphate, 2′-deoxyguanosine 5′-triphosphate, 2′-deoxycytidine 5′-triphosphate, dithiothreitol, lysozyme, SigmaUltra sucrose, and streptomycin sulfate were from Sigma (St. Louis, MO). Vivaspin centrifugal concentrators (molecular weight cutoff of 5000) were purchased from Vivascience Limited (Gloucestershire, U.K.). Sephadex G-100 and DEAE-Sepharose fast-flow were from Pharmacia Biotech (Piscataway, NJ). DEAE-cellulose DE52 was purchased from Whatman (Clifton, NJ). [γ-^{32}P]ATP (3000 Ci/mmol) was from PerkinElmer (Boston, MA). PEI-cellulose plates were from J. T. Baker (Phillipsburg, NJ). EcoLite (+) scintillation cocktail was from ICN Biomedicals Inc. (Costa Mesa, CA). All solvents and reagents were of the highest purity available, and buffers were treated with Chelex-100 before use to remove trace metals.

Preparation of MutT. The recombinant *E. coli* strain HMS174(DE3) (pETMutT) was used for the preparation of MutT, as previously described (*23*). The enzyme was purified to >95% homogeneity on the basis of SDS−PAGE.

Synthesis and Purification of 8-Oxo-dGTP and 8-Oxo-dGDP. 8-Oxo-dGTP and 8-oxo-dGDP were synthesized by a modification of the procedure of Mo et al. (*17*, *24*), by incubating 6 mM nucleotide in 100 mM sodium phosphate buffer (pH 6.8), 30 mM ascorbic acid, and 100 mM hydrogen peroxide in the dark at 37 °C for 3 h. The reaction mixture was then filtered through a 0.22 μm syringe filter and loaded onto a DEAE-cellulose column (2.5 cm × 15 cm) equilibrated with 20 mM TEAB[1] buffer (pH 8.5) at 4 °C. The column was eluted with a linear gradient from 20 to 160 mM TEAB. The fractions having UV spectra characteristic of 8-oxo-dG (two maxima at 247 and 293 nm) (*17*, *25*, *26*) were pooled and freeze-dried. The resulting 8-oxo nucleotides were ≥90% pure as determined by HPLC. They eluted as single peaks when chromatographed isocratically from a Phenomenex (Torrance, CA) C18 analytical column with a Beckman System Gold HPLC system, using 100 mM NaH_2PO_4-NaOH buffer (pH 5.5) and 10% methanol as the mobile phase, at a flow rate of 1 mL/min.

Synthesis of Radioactively Labeled 8-Oxo-dGTP. [γ-^{32}P]-8-Oxo-dGTP was prepared by transphosphorylation of 8-oxo-dGDP with [γ-^{32}P]ATP as previously reported (*15*). The labeled 8-oxo-dGTP was isolated by PEI-cellulose TLC with 0.6 M TEAB buffer (pH 8.5) as the mobile phase, and further purified by DEAE-cellulose column chromatography at 4 °C.

General Methods. The concentration of MutT was determined spectrophotometrically using an A_{280} of 2.2 for 1 mg/mL (*14*). Nucleotide concentrations were determined using the following extinction coefficients: $\epsilon_{252} = 1.37 \times 10^4$ M^{-1} cm^{-1} for dGTP (*14*), $\epsilon_{271} = 9.3 \times 10^3$ M^{-1} cm^{-1} for dCTP (*27*), and $\epsilon_{293} = 1.496 \times 10^4$ M^{-1} cm^{-1} for 8-oxo-dGTP and 8-oxo-dGDP (*17*, *26*).

Steady State Kinetic Studies. Steady state kinetic experiments with Mg^{2+}- or Mn^{2+}-activated MutT were performed by measuring the amount of dGMP or dCMP product released from the respective dNTPs in Tris-HCl buffer (50 mM, pH 7.5) at 23 °C. For convenience, the nucleotide products were quantitated by HPLC. After the reaction had been quenched with 0.3 M EDTA, aliquots (30−50 μL) of the reaction mixtures were chromatographed isocratically on a C18 analytical column using a Beckman HPLC system, and eluted as described above. Solutions with known nucleotide concentrations were used for calibration. In a test of the HPLC assay, the measured kinetic parameters for the MutT-catalyzed hydrolysis of dGTP were found to agree with those previously determined with the standard radioactive assay using [γ-^{32}P]dGTP (*14*).

Chemical-Quench Procedures. The pre-steady state time courses for the MutT-catalyzed hydrolysis of dGTP, dCTP, and 8-oxo-dGTP were measured using a KinTek RFQ-3 rapid chemical-quench-flow instrument from KinTek Corp. (State College, PA) (*22*). All solutions were made in 50 mM Tris-HCl buffer (pH 7.5) with either 20 mM $MgCl_2$ or 2.0 mM $MnCl_2$. A 15 μL volume of a buffered solution of MutT was rapidly mixed with 15 μL of a buffered solution of dNTP at 23 °C for varying time intervals ranging from 10 ms to several seconds before quenching with ≥90 μL of 0.3 M EDTA. For each time point, a control, free of enzyme, was run. Quenching with formic acid (25%, v/v) yielded very similar rates, but was not used because of the large backgrounds.

With dGTP and dCTP as substrates, the dGMP and dCMP products were analyzed by HPLC using the same conditions as in the steady state assay. The PP_i product of hydrolysis of [γ-^{32}P]-8-oxo-dGTP was analyzed by measuring the amount of labeled PP_i released (*14*). Charcoal [100 μL of a 20% (w/v) suspension] was added to the quenched samples (which ranged in volume from 120 to 260 μL), and the samples were incubated for 10 min on ice. After centrifugation, a 100 μL aliquot of the supernatant was dissolved in Ecolite scintillation cocktail (3.5 mL) and counted in a Beckman LS6000SE automatic liquid scintillation counter.

Analysis of the Transient Kinetic Data. The data from single-turnover experiments were initially fitted to single exponentials according to eq 2 using Grafit (Erithacus Software Ltd., Staines, U.K.)

$$Y = A(1 - e^{-k_{obs}t}) \quad (2)$$

where A and k_{obs} denote the amplitude and the observed rate constant, respectively, of the first-order appearance of product. Multiple-turnover data sets were initially fitted to the sum of a single first-order phase and a linear phase according to eq 3

$$Y = A(1 - e^{-k_{obs}t}) + k_{ss}t \quad (3)$$

where A and k_{obs} are as defined above and k_{ss} denotes the linear steady state rate constant. Global fitting of the single-turnover data, with Dynafit (Biokin Ltd., Pullman, WA) (*28*), to Scheme 2, a truncated portion of Scheme 1 containing an

[1] Abbreviations: HSQC, heteronuclear single-quantum coherence; TEAB, triethylammonium bicarbonate; TLC, thin-layer chromatography.

Scheme 2

$$\mathbf{F} \underset{k_{-5}}{\overset{k_5}{\rightleftharpoons}} \mathbf{E} + \mathrm{NTP} \underset{k_{-1}}{\overset{k_1}{\rightleftharpoons}} \mathbf{E{\bullet}NTP} \xrightarrow{k_2} \mathbf{E{\bullet}NMP{\bullet}PP_i}$$

enzyme isomerization step (k_5 and k_{-5}), yielded the rate constants k_1, k_{-1}, k_2, k_5, and k_{-5}. Next, global fitting of the multiple-turnover data to Scheme 1 with DynaFit, using the results of the single-turnover analysis, yielded the remaining rate constants k_3, k_{-3}, k_4, and k_{-4}. The quality of the fits may be judged by Figures 2, 4, and 6, and by the computed errors in the rate constants in Table 1. Finally, the rate constants obtained by transient state kinetics were used to calculate the steady state kinetic parameters k_{cat} and K_m for comparison of the two methods.

Effects of Viscocity on the k_{cat} of MutT-Catalyzed Reactions. To independently test for rate-limiting product dissociation, the effects of the microviscogen, sucrose (from 0 to 34%, w/v), on k_{cat} were studied essentially as described previously (*29*), initially at two high concentrations of the dNTP substrate to ensure saturation in both the absence and presence of sucrose. For Mg^{2+}-activated dGTPase, the final samples contained 3.0 mM dGTP, 20 mM $MgCl_2$, and 180 nM MutT. For Mn^{2+}-activated dGTPase, the final samples contained 3.0 mM dGTP, 5.0 mM $MnCl_2$, and 1.8 μM MutT. For Mg^{2+}-activated dCTPase, the final samples contained 12.0 mM dCTP, 20 mM $MgCl_2$, and 1.8 μM MutT. For Mg^{2+}-activated 8-oxo-dGTPase, the final samples contained 20 μM 8-oxo-dGTP, 20 mM $MgCl_2$, and 3.6 nM MutT. In addition, all samples contained 50 mM Tris-HCl (pH 7.5) and 1.0 unit of inorganic pyrophosphatase from baker's yeast per 50 μL of assay mixture. The enzymes were assayed colorimetrically at 23 °C as described previously (*16*). The data were analyzed as described in ref *29* by plotting the relative values of k_{cat} measured in the absence and presence of sucrose ($k_{cat}^{control}/k_{cat}^{sucrose}$) versus the relative viscosities of the sucrose-containing samples (η/η_0), which were calculated from the percentage of sucrose (w/v) using the handbook values (*30*). The data were fitted to a straight line, and the slopes are reported. Positive slopes indicate inhibitory effects of sucrose on k_{cat}, while negative slopes indicate activating effects (*29*).

RESULTS AND DISCUSSION

Single-Turnover Kinetics of Mg^{2+}-Activated MutT with dGTP as the Substrate. The rapid chemical-quench method was used to examine the pre-steady state kinetics of the MutT-catalyzed hydrolysis of dGTP, the most extensively studied substrate of the MutT reaction (*9*, *10*). Single-turnover experiments with MutT in excess over the nucleotide substrate allowed measurement of the rate constants for substrate binding (k_1) and dissociation (k_{-1}) and the chemical step (k_2). With MutT in excess, dGTP was hydrolyzed in a single pass through the enzymatic pathway. Thus, the kinetics were free of complications resulting from the steady state formation of products.

Figure 2A shows the time course for single-turnover hydrolysis of dGTP at four concentrations of MutT. The curves in Figure 2A are the results of global fitting of the data to Scheme 2, a truncated portion of Scheme 1, with DynaFit (*28*). This analysis yielded k_1, k_{-1}, k_2, k_5, and k_{-5} (Table 1). To justify the use of Scheme 2, the data were initially fitted by nonlinear least-squares methods to single exponentials to yield the pseudo-first-order rate constants, k_{obs}, at each concentration of MutT. In the range of MutT concentrations that were used, k_{obs} was found to increase linearly with enzyme concentration. The apparent second-order rate constant for dGTP binding, k_{on}^{app}, was estimated from the slope of the line to be $(1.0 \pm 0.1) \times 10^4$ M^{-1} s^{-1}, a value far below the diffusion limit of $\sim 10^9$ M^{-1} s^{-1}.

The unusually low value of k_{on}^{app} provides independent support for an iso mechanism for MutT (Schemes 1 and 2 and Figure 1), as originally suggested by product inhibition studies (*17*), justifying the global fitting of the single-turnover data to Scheme 2.[2] Noncompetitive product inhibition by dGMP implied that MutT might undergo a conformational change from E to F during the reaction (k_3), which was slowly reversed in the free enzyme (k_5) before the next substrate molecule could bind. Thus, the apparent rate constant for dGTP binding (k_{on}^{app}) should be

$$k_{on}^{app} = (k_1 k_5)/(k_5 + k_{-5}) \quad (4)$$

The true rate constant (k_1) for binding of dGTP to E, the active form of MutT, obtained from the global fit, is 1.9×10^6 M^{-1} s^{-1}, 3 orders of magnitude below the diffusion limit. The rate constants k_5 and k_{-5} for the reversible isomerization of MutT were computed to be 12.1 and 300 s^{-1}, respectively. The apparent second-order rate constant for dGTP binding, independently calculated with eq 4 from these values of k_1, k_5, and k_{-5} [$k_{on}^{app} = (7.2 \pm 2.2) \times 10^4$ M^{-1} s^{-1}], was of the same order of magnitude as that estimated from the slope of the line relating k_{obs} to enzyme concentration [$(1.0 \pm 0.1) \times 10^4$ M^{-1} s^{-1}]. The rate constant for the chemical step (k_2) found by the global fit was 10.7 s^{-1} (Table 1), which is faster than k_{cat} (4.0 s^{-1}, Table 2) (*14*), consistent with the need for an additional partially rate-limiting step.

Multiple-Turnover Kinetics of Mg^{2+}-Activated MutT with dGTP as the Substrate. Figure 2B shows the time course of multiple-turnover experiments with 60 μM MutT and excess dGTP ranging from 0.15 to 1.2 mM, in the presence of 20 mM $MgCl_2$. The curves are the results of global fitting of the data to Scheme 1, using the results of the single-turnover fit. This analysis yielded the remaining rate constants k_3, k_{-3}, k_4, and k_{-4} (Table 1). The time course of dGMP formation was biphasic with an initial burst corresponding to the first turnover during which dGMP formed rapidly, followed by a slower rate of product formation (the linear phase) corresponding to the steady state turnover (*22*). The burst of product formation indicated the presence of one or more rate-limiting steps following the chemical step (k_2), justifying the use of Scheme 1.

From the global fitting of the single-turnover data to Scheme 2, the rate constant (k_5) for the isomerization of MutT from the product-binding form F to the substrate-binding

[2] Analysis of the single-turnover data with only three rate constants (k_1, k_{-1}, and k_2) instead of five yields larger sums of squares of residual errors in all cases: for Mg^{2+}-activated dGTP hydrolysis, 7.4×10^{-7} and 6.1×10^{-7} μM^2 for three and five rate constants, respectively; for Mn^{2+}-activated dGTP hydrolysis, 9.6×10^{-7} and 7.1×10^{-7} μM^2, respectively; and for Mg^{2+}-activated 8-oxo-dGTP hydrolysis, 3.3×10^{-11} and 2.7×10^{-11} μM^2, respectively. More seriously, the fits with only three rate constants provide no explanation of the slow rate constants measured for substrate binding (k_{on}^{app}) in all cases.

Table 1: Rate Constants of the MutT-Catalyzed Hydrolysis of dGTP and 8-Oxo-dGTP[a]

		dGTP		8-oxo-dGTP
reaction	rate constant	Mg^{2+}-activated	Mn^{2+}-activated	Mg^{2+}-activated
E + NTP ⇌ E·NTP	k_1 (M^{-1} s^{-1})	$(1.9 \pm 0.3) \times 10^6$	$(1.7 \pm 0.2) \times 10^6$	$(7.5 \pm 0.1) \times 10^8$
	k_{-1} (s^{-1})	120 ± 50	1.4 ± 0.1	2.6 ± 0.4
E·NTP → E·NMP·PP_i	k_2 (s^{-1})	10.7 ± 0.6	1.21 ± 0.02	32.3 ± 0.2
E·NMP·PP_i ⇌ F·NMP + PP_i	k_3 (s^{-1})	480 ± 160	550 ± 90	160 ± 60
	k_{-3} (M^{-1} s^{-1})	$(2.3 \pm 0.5) \times 10^7$	$(9.1 \pm 1.4) \times 10^7$	$(1.3 \pm 0.5) \times 10^9$
F·NMP ⇌ F + NMP	k_4 (s^{-1})	70 ± 20	6.8 ± 0.2	3.9 ± 1.1
	k_{-4} (M^{-1} s^{-1})	$(1.5 \pm 0.2) \times 10^4$	$(1.0 \pm 0.2) \times 10^4$	$(4.6 \pm 1.0) \times 10^7$
F ⇌ E	k_5 (s^{-1})	12.1 ± 0.6	2.1 ± 0.1	12.1 ± 5.2
	k_{-5} (s^{-1})	300 ± 80	12 ± 4	300 ± 240

[a] Conditions: 50 mM Tris, 20 mM $MgCl_2$, or 2.0 mM $MnCl_2$, pH 7.5, and 23 °C. These kinetic constants and their errors were obtained from the best fits of the transient state kinetic data to Scheme 1 with DynaFit (*28*).

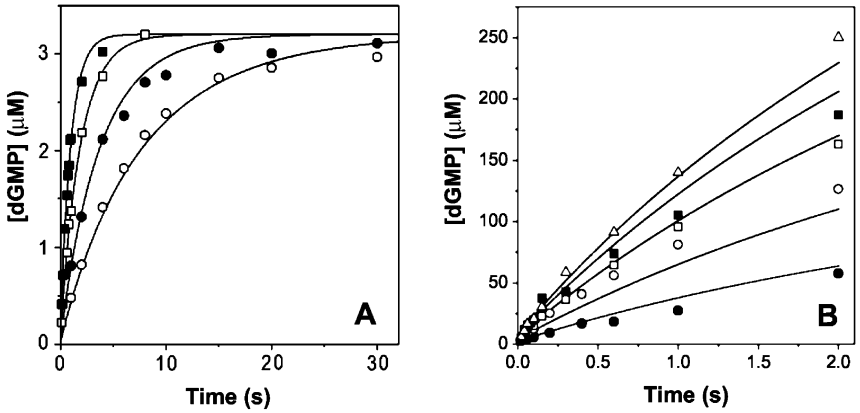

FIGURE 2: Transient kinetics of the MutT-catalyzed hydrolysis of dGTP with Mg^{2+} as the activator. (A) Single-turnover hydrolysis of dGTP. Excess MutT concentrations were mixed with dGTP (3.2 μM) to initiate the reaction in the presence of 20 mM $MgCl_2$ and 50 mM Tris-HCl (pH 7.5) at 23 °C, and the reactions were quenched with 0.3 M EDTA at time intervals ranging from 10 ms to 30 s. All reported concentrations are those after mixing in the rapid quench instrument. The MutT concentrations were 15 (○), 30 (●), 60 (□), and 120 μM (■). The curves are from global fitting of the data to the mechanism in Scheme 2 with DynaFit (*28*) which yielded the rate constants k_1, k_{-1}, k_2, k_5, and k_{-5} given in Table 1, as described in Experimental Procedures. (B) Multiple-turnover hydrolysis of dGTP. Pre-steady state time courses of the MutT-catalyzed hydrolysis of dGTP [0.15 (●), 0.3 (○), 0.6 (□), 0.9 (■), and 1.2 mM (△)] in the presence of 20 mM $MgCl_2$, 60 μM MutT, and 50 mM Tris-HCl (pH 7.5) at 23 °C. The curves are from global fitting of the data to the mechanism shown in Scheme 1 which yielded the rate constants k_3, k_{-3}, k_4, and k_{-4} given in Table 1.

Table 2: Comparison of Constants from Transient State and Steady State Kinetics[a]

		dGTP		8-oxo-dGTP
experiment	rate constant	Mg^{2+}-activated	Mn^{2+}-activated	Mg^{2+}-activated
transient state	k_{cat} (s^{-1})[b]	5.2 ± 2.5	0.69 ± 0.16	2.6 ± 0.4
	K_m (μM)[c]	880 ± 500	6.0 ± 2.4	0.10 ± 0.03
	k_{on}^{app} (M^{-1} s^{-1})[d]	$(1.0 \pm 0.1) \times 10^4$	$(2.2 \pm 0.2) \times 10^5$	$(3.2 \pm 0.2) \times 10^7$
	k_{on}^{app} (M^{-1} s^{-1})[e]	$(7.2 \pm 2.2) \times 10^4$	$(2.4 \pm 0.9) \times 10^5$	$(2.8 \pm 0.7) \times 10^7$
steady state	k_{cat} (s^{-1})	4.0 ± 0.1	0.23 ± 0.04[f]	2.8 ± 0.2
	K_m (μM)	280 ± 80	6.3 ± 0.5	0.52 ± 0.05
	k_{cat}/K_m (M^{-1} s^{-1})	$(1.4 \pm 0.4) \times 10^4$	$(4.1 \pm 0.4) \times 10^4$	$(5.4 \pm 0.7) \times 10^6$

[a] Conditions: 50 mM Tris, 20 mM $MgCl_2$, or 2.0 mM $MnCl_2$, pH 7.5, and 23 °C. [b] k_{cat} was calculated with eq 5. [c] K_m was calculated with the equation $K_m = k_4(k_5 + k_{-5})(k_{-1}k_3 + k_2k_3)/k_1(k_2k_3k_4 + k_2k_3k_5 + k_2k_4k_5 + k_3k_4k_5)$ (*18*). [d] k_{on}^{app} was estimated from the initial slope of the plot of the MutT concentration-dependent k_{obs} values from single-turnover kinetics. [e] k_{on}^{app} was calculated with eq 4. [f] This k_{cat} value is the average of that previously reported (0.19 s^{-1}) (*14*) and a more recent measurement (0.26 s^{-1}).

form E was 12.1 s^{-1}, a value close to that of the partially rate-limiting chemical step (k_2 = 10.7 s^{-1}) (Table 1). Therefore, the isomerization of MutT is a partially rate-limiting step following the hydrolytic step in the enzymatic pathway.

Other possible rate-limiting steps might be the release of the products (Scheme 1). Product inhibition studies suggested that PP_i was the first product to leave, followed by dGMP (*17*). A relatively minor contribution of product release to rate limitation is suggested by the small inhibitory effect on k_{cat} of increasing the relative microviscosity with sucrose (Figure 3), yielding a positive slope of 0.18 ± 0.02.[3] The release of PP_i is unlikely to be significantly rate-limiting because of its high inhibitor constant, suggesting weak binding ($K_I^{intercept}$ = 5.0 mM) (*17*). Global fitting of the multiple-turnover data to Scheme 1 confirmed the fast release of PP_i (k_3 = 480 s^{-1}) (Table 1).

[3] At 37 °C, no effects of the microviscogens, sucrose or glycerol [0−40% (w/v)], were observed on k_{cat} of the dGTPase reaction catalyzed by Mg^{2+}-activated MutT (*15*). Hence, the effects of increasing viscosity on k_{cat} are strongly temperature dependent.

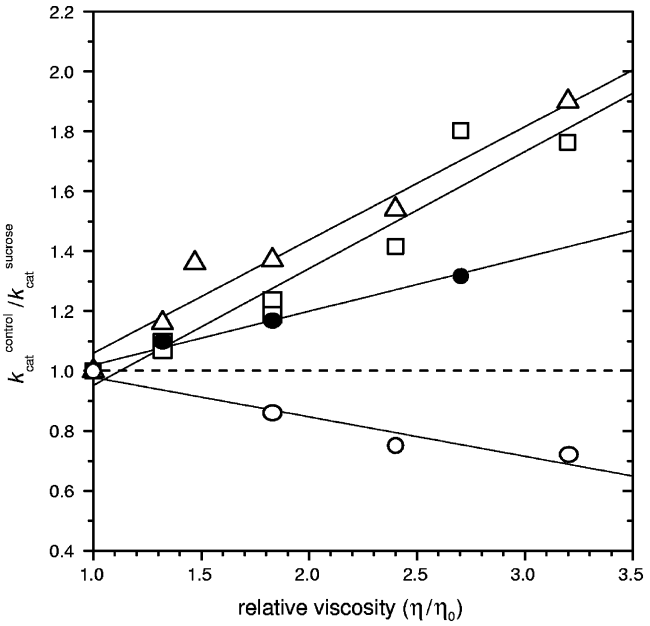

FIGURE 3: Effects of increasing viscocity induced by sucrose on k_{cat} of the MutT reaction. Plot, according to Cole et al. (*29*), of the relative k_{cat} vs relative viscocity in the Mg^{2+}-activated MutT-catalyzed hydrolysis of dGTP (●), dCTP (○), and 8-oxo-dGTP (△), and the Mn^{2+}-activated MutT-catalyzed hydrolysis of dGTP (□). Each point represents the average of two or three experiments. The slopes of the straight lines fitted to the data are 0.18 ± 0.02, -0.13 ± 0.03, 0.38 ± 0.04, and 0.39 ± 0.05, respectively. Conditions are given in Experimental Procedures.

The release of dGMP is also unlikely to be significantly rate-limiting since $^1H-^{15}N$ HSQC titration of MutT with dGMP in the presence of Mg^{2+} showed the binding of dGMP to induce stepwise changes in backbone ^{15}N and/or ^{15}NH chemical shifts of 22 residues, indicating weak binding and fast exchange of free dGMP with enzyme-bound dGMP (*17*). The smallest chemical shift differences between the resonances of free MutT and the MutT−dGMP complex set a lower limit on the exchange rate constant ($k_{ex} = k_4 + k_{-4}$[dGMP] ≥ 598 s^{-1}). The NMR data also yielded the dissociation equilibrium constant for dGMP ($k_4/k_{-4} = 1.8$ mM). Solving these two simultaneous equations yielded a k_4 of ≥ 74.5 s^{-1} and a k_{-4} of $\geq 4.2 \times 10^4$ M^{-1} s^{-1} solely from the NMR data (*17*). These values are fast compared to k_{cat} (4.0 s^{-1}, Table 2) (*14*). Moreover, they show reasonable agreement with the rate constants k_4 and k_{-4} obtained by global fitting of the multiple-turnover experiments to Scheme 1 for Mg^{2+}-activated dGTP hydrolysis (Table 1), indicating that the release of the product dGMP is not strongly rate-limiting.

Very small contributions of the product release steps, k_3 and k_4, to rate limitation are also indicated by a calculation of the k_{cat} for steady state turnover from the individual rate constants of Table 1 using the general equation (eq 5) derived for Scheme 1 (*18*).

$$k_{cat} = (k_2k_3k_4k_5)/(k_2k_3k_4 + k_2k_3k_5 + k_2k_4k_5 + k_3k_4k_5) \quad (5)$$

The k_{cat} of 5.2 s^{-1}, calculated with eq 5, is in good agreement with the k_{cat} of 4.0 s^{-1}, determined experimentally by steady state kinetic analysis (*14*). The same value for k_{cat} (5.2 s^{-1}) is calculated with eq 6, which was derived from eq 5 by assuming fast dissociation (k_3) of PP_i from the product complex

$$k_{cat} = (k_2k_4k_5)/(k_2k_4 + k_2k_5 + k_4k_5) \quad (6)$$

but an 8% higher k_{cat} of 5.6 s^{-1} is calculated with eq 7 which assumes fast dissociation (k_4) of dGMP.

$$k_{cat} = (k_2k_3k_5)/(k_2k_3 + k_2k_5 + k_3k_5) \quad (7)$$

If the rate constants for the dissociation of PP_i (k_3) and dGMP (k_4) are both fast, eq 5 simplifies to eq 8 which contains *only* the rate constants of the chemical step (k_2) and the isomerization step (k_5).

$$k_{cat} = (k_2k_5)/(k_2 + k_5) \quad (8)$$

The k_{cat} for steady state turnover calculated with eq 8 increased by 10% to 5.7 s^{-1}. The small increases in k_{cat} calculated with eqs 7 and 8 reflect the major contributions of k_2 and k_5 to rate limitation with only a very small contribution of dGMP release (k_4). Hence, the major partially rate-limiting step following the hydrolysis of dGTP (k_2) found by the multiple-turnover experiments is the isomerization of MutT from F to E (k_5), providing further independent evidence for an iso kinetic mechanism (Scheme 1). Partial rate limitation by the chemical step (k_2) is consistent with the pH dependence of k_{cat} (*15*) and the 1.8 ± 0.3-fold solvent deuterium kinetic isotope effect on k_{cat} (*10*).

Single-Turnover Kinetics of Mn^{2+}-Activated MutT with dGTP as the Substrate. Steady state kinetic analysis (*14*) showed that replacing Mg^{2+} with Mn^{2+} altered the hydrolytic activity of MutT with dGTP, decreasing both k_{cat} and K_m. While the k_{cat} of Mg^{2+}-activated MutT was 4.0 s^{-1} and the K_m was 0.28 mM, the Mn^{2+}-activated enzyme had a 17-fold lower k_{cat} (0.23 s^{-1}), and a 44-fold lower K_m (6.3 μM) (*14*) (Table 2).

Figure 4A shows the time course of single-turnover experiments with 5 μM dGTP at four concentrations of MutT ranging from 15 to 39 μM in the presence of 2.0 mM $MnCl_2$. The highest enzyme concentration used was shown to be saturating by a separate measurement of k_{obs} at 59 μM enzyme. The curves are the results of global fitting of the data to Scheme 2, yielding the rate constants k_1, k_{-1}, k_2, k_5, and k_{-5} (Table 1).[2] The use of Scheme 2 was initially justified by calculating k_{obs}, obtained by exponential fitting of the single-turnover data at each MutT concentration. The values of k_{obs} as a function of MutT concentration were fitted to a hyperbola, permitting the evaluation of k_{obs} at saturating enzyme concentrations where $k_{obs} = k_2$, the rate constant for the chemical step. The k_2 thus obtained with Mn^{2+} activation (1.21 s^{-1}) is 8.8-fold lower than that obtained with Mg^{2+} activation (Table 1). The apparent second-order rate constant for dGTP binding (k_{on}^{app}), estimated from the initial slope of the hyperbola as 2.2×10^5 M^{-1} s^{-1}, was much slower than the diffusion limit of $\sim 10^9$ M^{-1} s^{-1}, suggesting that partially rate-limiting isomerization of MutT also occurs with Mn^{2+} as the activator. Accordingly, the global fitting of the single-turnover data to Scheme 2 yielded k_1, the rate constant for dGTP binding of 1.7×10^6 M^{-1} s^{-1} (Table 1). This value of k_1 for Mn^{2+}-activated MutT agrees with the k_1 found with Mg^{2+}-activated MutT (Table 1), consistent with the formation

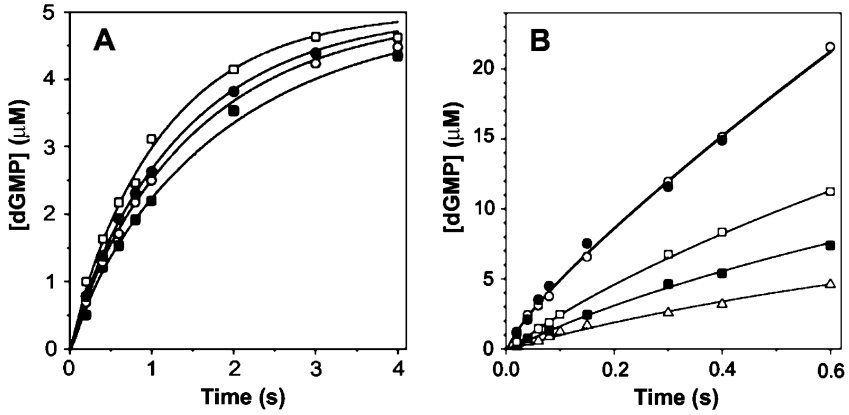

FIGURE 4: Transient kinetics of the MutT-catalyzed hydrolysis of dGTP with Mn^{2+} as the activator. (A) Single-turnover hydrolysis of dGTP. A solution of dGTP (5 μM) was mixed with increasing concentrations of MutT to initiate the reaction in the presence of 2.0 mM $MnCl_2$ and 50 mM Tris-HCl (pH 7.5) at 23 °C. The MutT concentrations were 15 (■), 20 (○), 24 (●), and 39 μM (□). The curves are from global fitting of the data to the mechanism in Scheme 2 which yielded the rate constants k_1, k_{-1}, k_2, k_5, and k_{-5} given in Table 1. (B) Multiple-turnover hydrolysis of dGTP. Pre-steady state time courses of the MutT-catalyzed hydrolysis of dGTP [10 (△), 18 (■), 30 (□), 600 (○), and 900 μM (●)] in the presence of 2.0 mM $MnCl_2$, 60 μM MutT, and 50 mM Tris-HCl (pH 7.5) at 23 °C. The curves are from global fitting of the data to the mechanism shown in Scheme 1, which yielded the rate constants k_3, k_{-3}, k_4, and k_{-4} given in Table 1.

of a second-sphere dGTP complex rather than an inner-sphere complex with the enzyme-bound divalent cation (Figure 1) (*12*).

The global fit also yielded a rate constant k_5 of 2.1 s^{-1} for the iso step from F to E, and a rate constant k_{-5} of 12 s^{-1} for the reverse isomerization. Thus, with Mn^{2+} as the activator, the isomerization rate constant decreased 5.8-fold, and the reverse rate constant decreased 25-fold (Table 1). These significantly lower rate constants for enzyme isomerization, and its reverse, on changing *only* the divalent cation activator from Mg^{2+} to Mn^{2+} suggest that the isomerization involves a change in metal coordination, as indicated in the chemical mechanism of Figure 1. The computed values of k_1, k_5, and k_{-5} yielded, with eq 4, a value of 2.4×10^5 M^{-1} s^{-1} for k_{on}^{app} which agrees with the value of 2.2×10^5 M^{-1} s^{-1} directly estimated from the initial slope of the MutT concentration dependence of k_{obs} (Table 2).

Multiple-Turnover Kinetics of Mn^{2+}-Activated MutT with dGTP as the Substrate. Figure 4B shows the time courses of multiple-turnover experiments with 60 μM MutT in the presence of 2.0 mM $MnCl_2$ and dGTP concentrations ranging from 10 to 900 μM. The curves are the results of global fitting of the data to Scheme 1, using the results of the single-turnover fit. This analysis yielded the remaining rate constants k_3, k_{-3}, k_4, and k_{-4} (Table 1). The burst of product formation in the initial turnover, most notably at 600 and 900 μM dGTP, suggested the presence of one or more rate-limiting steps following the chemical step of dGTP hydrolysis (k_2).

Product release steps are unlikely to be totally rate-limiting on the basis of product inhibition studies (*17*), which showed a K_I^{slope} for dGMP of 4.0 mM, a $K_I^{intercept}$ for dGMP of 4.6 mM, and a $K_I^{intercept}$ for PP_i of 0.4 mM. Since the single-turnover data showed the isomerization rate constant k_5 to be slow, this step may well be partially rate-limiting during steady state turnover, justifying the use of Scheme 1.

The k_{cat} calculated with eq 5 from the rate constant of the chemical step (k_2), the product release steps (k_3 and k_4), and the enzyme isomerization step (k_5) was 0.69 s^{-1}, which is comparable to the experimental value of 0.23 ± 0.04 s^{-1} obtained by steady state measurements (Table 2). The same value of k_{cat} (0.69 s^{-1}) is calculated with eq 6 which assumes fast dissociation of PP_i, while 12% higher values of k_{cat} (0.77 s^{-1}) are calculated with eq 7, which assumes fast dissociation (k_3) of dGMP, and with eq 8 which assumes fast dissociation of both PP_i and dGMP (k_4). These results are consistent with major rate limitation by the chemical and iso steps, with a smaller contribution from dGMP release. Accordingly, a significant inhibitory effect on k_{cat} was found with an increase in the relative microviscosity with sucrose (Figure 3), yielding a slope of 0.39 ± 0.05, consistent with partially rate-limiting dGMP release. The rate constants obtained by the transient state kinetic methods generally show reasonable agreement with those obtained by steady state kinetics (Table 2).

The dependence of the rate constants of the iso step (k_5), and its reverse (k_{-5}), on the species of divalent cation used as the activator is consistent with the proposed chemical mechanism of the iso step which involves ligand substitution on the enzyme-bound metal (Figure 1). In this mechanism, $M^{2+}PP_i$ becomes directly coordinated to the enzyme-bound divalent cation in the chemical step (k_2), and is subsequently displaced from the metal by Glu-53 (k_3), thereby converting E to F. In the next step (k_4), dGMP dissociates, leaving the altered form of the enzyme F. The slow dissociation of Glu-53 from the enzyme-bound divalent cation (k_5), facilitated by Glu-98, prior to the binding of the next dGTP substrate, constitutes the partially rate-limiting iso step. The F form of MutT is inactive for two reasons: (i) it cannot productively bind the NTP substrate, and (ii) Glu-53, which is coordinated by the enzyme-bound divalent cation, cannot function as the general base. In the isomerization of F to E (k_5), Glu-53 is replaced in the metal coordination sphere with Glu-98, permitting the next dGTP substrate to bind, and Glu-53 to deprotonate the water nucleophile (Figure 1) (*15*, *17*). Hence, the slower rate constants (k_5 and k_{-5}) for enzyme isomerization with Mn^{2+} likely result from the slower dissociation of the Glu-53 and Glu-98 ligands from the coordination sphere of Mn^{2+} than from Mg^{2+} (Table 1).

Multiple-Turnover Measurements of Mg^{2+}-Activated MutT with dCTP as the Substrate. The rate constant for the isomerization of MutT (k_5), and its reverse (k_{-5}), should be

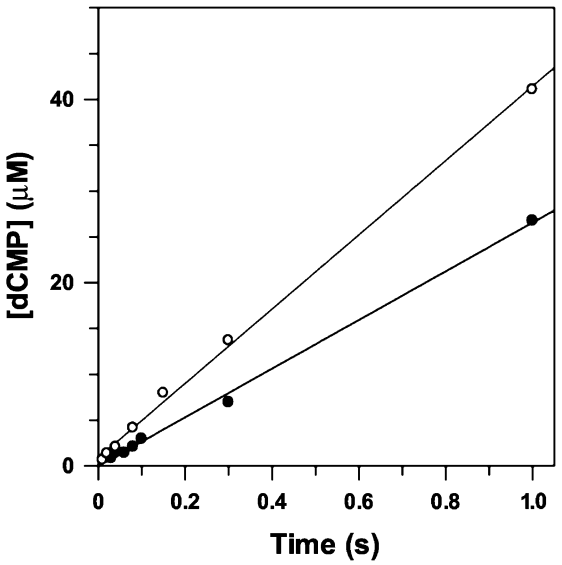

FIGURE 5: Multiple-turnover hydrolysis of dCTP catalyzed by Mg^{2+}-activated MutT. A solution of MutT (120 μM) was mixed with dCTP at 2.18 (●) and 3.64 mM (○), in the presence of 20 mM $MgCl_2$ and 50 mM Tris-HCl (pH 7.5) at 23 °C. Note the absence of a burst in the formation of dCMP. The lines represent linear fits of the data. The steady state k_{cat} of 0.33 s^{-1} was calculated from the maximal ratio of the slope divided by the enzyme concentration.

independent of the substrate, if the divalent cation activator is not changed. With Mg^{2+}-activated MutT, dCTP is a poor substrate with a steady state k_{cat} of 0.58 ± 0.08 s^{-1} and a K_m of 1.2 ± 0.3 mM. This k_{cat} is 6.9-fold lower than that of dGTP (4.0 s^{-1}) and 20.9-fold lower than the isomerization rate constant of MutT in the presence of Mg^{2+} (k_5 = 12.1 s^{-1}). Since product release is expected to be rapid for the reasons given above, the hydrolysis of dCTP should not show a burst, since there are no rate-limiting steps following the slow chemical step (k_2). As an independent test of the iso mechanism of Scheme 1, multiple-turnover experiments were carried out with dCTP as the substrate and Mg^{2+} as the activator. Unlike the multiple-turnover hydrolysis of dGTP (Figure 2B), no burst of product formation was observed in the kinetics of dCTP hydrolysis (Figure 5), indicating the absence of rate-limiting steps following the chemical step (k_2). Hence, the steady state rate of the MutT-catalyzed hydrolysis of dCTP is limited by the chemical step, while the product release steps (k_3 and k_4) and the isomerization step (k_5) must be at least 1 order of magnitude faster. A k_{cat} value of 0.33 s^{-1} was calculated from the multiple-turnover experiments as the maximal ratio of the slope divided by the enzyme concentration, at the highest level of dCTP (3.64 mM) which could be used (Figure 5). Higher levels of dCTP gave unacceptably large backgrounds. The calculated k_{cat} showed reasonable agreement with the experimental value of 0.58 s^{-1} found via the steady state kinetic assay at a much lower enzyme concentration. Consistent with rate-limiting chemistry alone, increasing the microviscosity with sucrose did not decrease k_{cat} of the dCTPase reaction but slightly increased it (Figure 3), yielding a negative slope of −0.13 ± 0.03. Such small inverse effects of sucrose on k_{cat} have previously been found with the human C-terminal Src protein kinase with the poor substrate ATPγS, and are unexplained. They may reflect nonspecific actvation of the enzyme by the viscogen (*29*).

Single-Turnover Kinetics of Mg^{2+}-Activated MutT with 8-Oxo-dGTP as the Substrate. As found by steady state kinetics at pH 7.5 and 23 °C, the catalytic efficiency (k_{cat}/K_m) of Mg^{2+}-activated MutT with 8-oxo-dGTP as the substrate (5.4 × 10^6 M^{-1} s^{-1}) is 385-fold higher than that with dGTP as a result of the 540-fold lower K_m for 8-oxo-dGTP (*14*, *16*) (Table 2). While the steady state kinetic analysis shows only a lower K_m for 8-oxo-dGTP, expressions derived for K_m in an iso mechanism contain no fewer than seven rate constants (Table 2) (*18*). Pre-steady state kinetics can provide the individual rate constants for all steps in the kinetic mechanism and thereby elucidate detailed changes in rate-limiting steps.

Figure 6A shows time courses for single-turnover hydrolysis of 14 nM 8-oxo-dGTP with varying excess MutT concentrations ranging from 0.16 to 1.1 μM in the presence of 20 mM $MgCl_2$. The curves are the results of global fitting of the data to Scheme 2,[2] making the reasonable assumption that the rate constants for the isomerization of free enzyme (k_5) and its reverse (k_{-5}) were the same as those found with dGTP.[4] This analysis yielded the rate constants k_1, k_{-1}, k_2, k_5, and k_{-5} (Table 1). The use of Scheme 2 was justified by estimating k_{on}^{app}, from the initial slope of the effect of MutT concentration on k_{obs} for product (PP_i) formation, to be 3.2 × 10^7 M^{-1} s^{-1}, a value below the diffusion limit. From the global fit, the rate constant for binding of 8-oxo-dGTP to the E form of MutT (k_1 = 7.5 × 10^8 M^{-1} s^{-1}) closely approaches the diffusion limit of ∼10^9 M^{-1} s^{-1}, and is 395-fold faster than the k_1 found for dGTP, indicating that the E-form of MutT is well adapted to efficiently bind its preferred substrate, 8-oxo-dGTP. Consistent with tighter binding, the rate constant for the dissociation of 8-oxo-dGTP from the enzyme complex (k_{-1} = 2.6 s^{-1}) is 46-fold slower than that of dGTP (Table 1). These results provide a detailed explanation of why 8-oxo-dGTP is a better substrate than dGTP at low substrate concentrations.

The rate constant for the chemical step from the global fitting (k_2 = 32.3 s^{-1}) is 3.0-fold faster than that found with dGTP and 11.5-fold faster than the steady state k_{cat} value of 8-oxo-dGTP (2.8 s^{-1}). Unlike the case of dGTP hydrolysis, where chemistry is partially rate-limiting, the chemical step (k_2) contributes little to rate limitation in the MutT-catalyzed hydrolysis of 8-oxo-dGTP, but steps after k_2 are rate-limiting (see below).

Since k_1 and k_{-1} are now known for both dGTP and 8-oxo-dGTP, we can now calculate and compare the true dissociation constants (k_{-1}/k_1) of these substrates from the active form E of MutT. These dissociation constants are 62 μM and 3.5

[4] The values of k_5 (12.1 ± 0.6 s^{-1}) and k_{-5} (300 ± 80 s^{-1}) for Mg^{2+}-activated dGTP hydrolysis were deemed more accurate than those obtained with 8-oxo-dGTP from more limited single-turnover data at ∼10^2-fold lower enzyme and substrate concentrations (k_5 = 17.3 ± 1.3 s^{-1} and k_{-5} = 46 ± 17 s^{-1}). With dGTP, the rates were slower, permitting the collection of more early data points, and more experiments were conducted. With 8-oxo-dGTP, the computed errors in k_5 and k_{-5} (7.7 and 36.1%, respectively) were significantly larger than those with dGTP (4.6 and 25.3%, respectively). Moreover, while the k_5 and k_{-5} values obtained with dGTP gave good fits to the 8-oxo-dGTPase data in both single- and multiple-turnover experiments, the k_5 and k_{-5} values obtained with 8-oxo-dGTP gave unacceptably poor fits to the single- and multiple-turnover experiments with both 8-oxo-dGTP and dGTP. The above differences in values and errors for k_5 and k_{-5} were taken into account in the larger errors given in Table 1 for k_5 and k_{-5} for 8-oxo-dGTP.

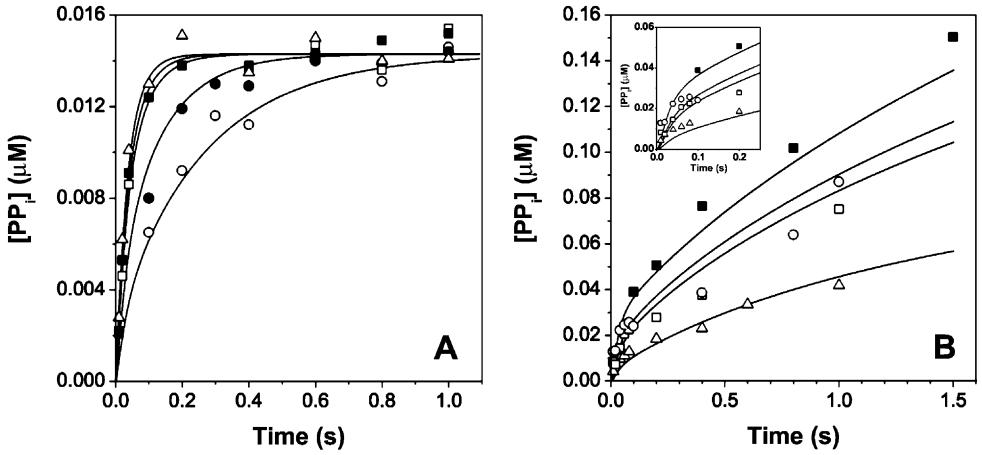

FIGURE 6: Transient kinetics of the MutT-catalyzed hydrolysis of 8-oxo-dGTP with Mg^{2+} as the activator. (A) Single-turnover hydrolysis of 8-oxo-dGTP. A solution of 8-oxo-dGTP, yielding a final substrate concentration of 0.014 μM, was mixed with increasing final concentrations of MutT [0.16 (○), 0.32 (●), 0.63 (□), 0.79 (■), and 1.1 μM (△)] in the presence of 20 mM $MgCl_2$ and 50 mM Tris-HCl (pH 7.5) at 23 °C. The curves are from global fitting of the data to the mechanism in Scheme 2, which yields the rate constants k_1, k_{-1}, k_2, k_5, and k_{-5} given in Table 1. (B) Multiple-turnover hydrolysis of 8-oxo-dGTP. A solution of MutT yielding a final enzyme concentration of 0.062 μM was mixed with increasing final concentrations of 8-oxo-dGTP [0.13 (△), 0.43 (□), 0.56 (○), and 1.17 μM (■)] in the presence of 20 mM $MgCl_2$ and 50 mM Tris-HCl (pH 7.5) at 23 °C. The inset expands the first 200 ms. The curves are from global fitting of the data to the mechanism shown in Scheme 1, which yielded the rate constants k_3, k_{-3}, k_4, and k_{-4} given in Table 1. The fits to the multiple-turnover data were improved by allowing the substrate concentrations to vary within their experimental errors, and by using a value for k_1 which was 53% of that found from the single-turnover data.

nM for dGTP and 8-oxo-dGTP, respectively. Thus, 8-oxo-dGTP binds to MutT with an affinity 1.8×10^4-fold greater than that of dGTP, corresponding to a 5.8 kcal/mol more favorable free energy of binding. Interestingly, this value is very similar to the ratio of the true dissociation constants found for the binding of the products dGMP ($K_D = 1.8$ mM) and 8-oxo-dGMP ($K_D = 52$ nM) to MutT by NMR titration and by isothermal titration calorimetry, respectively (*17*). Here as well, the ratio of affinities is 3.4×10^4, corresponding to a 6.1 kcal/mol more favorable free energy of binding of 8-oxo-dGMP than of dGMP. This entire difference in affinity for 8-oxo-dGMP versus dGMP has been shown by structural (*13*) and mutational studies (*16*) to result from hydrogen bonding interactions of the N7H and C8═O groups of 8-oxo-dGMP with Asn-119, and of the C8═O group of 8-oxo-dGMP with Arg-78 of MutT. The binding of 8-oxo-dGMP to a single site on MutT was also accompanied by a diffuse conformational change which altered the backbone ^{15}N and/or ^{15}NH chemical shifts of 62 residues (*17*), and greatly slowed the ^{15}NH exchange with D_2O of 45 residues widely distributed throughout the protein (*13*). The solution structure of the MutT−Mg^{2+}−8-oxo-dGMP complex also showed a significant narrowing of the nucleotide-binding cleft when compared with that of the free enzyme, and with that of the enzyme complexed with the $10^{3.7}$-fold weaker binding substrate analogue, Mg^{2+}AMPCPP (*12*, *13*).

Multiple-Turnover Kinetics of Mg^{2+}-Activated MutT with 8-Oxo-dGTP as the Substrate. With Mg^{2+}-activated MutT (62 nM) and excess 8-oxo-dGTP ranging from 0.13 to 1.2 μM, in the presence of 20 mM $MgCl_2$, a rapid burst of product (PP_i) formation was observed in the first 100 ms (Figure 6B). The curves are the results of global fitting of the data to Scheme 1, using the results of the single-turnover fit. This analysis yielded the remaining rate constants k_3, k_{-3}, k_4, and k_{-4} (Table 1). Faster burst rates with 8-oxo-dGTP than with dGTP were found, due to both the faster chemical step (k_2) and the similar slow rates of steady state turnover. Because of the fast chemical step in the hydrolysis of 8-oxo-dGTP, all of the rate-limiting steps follow the chemical step (Table 1). With Mg^{2+}-activated dGTP hydrolysis, the rate constant of the iso step ($k_5 = 12.1$ s^{-1}) was the only major rate-limiting step following the chemical step ($k_2 = 10.7$ s^{-1}). With 8-oxo-dGTP hydrolysis, the chemical step is faster ($k_2 = 32.3$ s^{-1}) and exceeds the steady state k_{cat} value of 2.8 s^{-1} by a factor of 11.5 (*16*).

Because of the fast chemical step found with 8-oxo-dGTP, the isomerization step alone ($k_5 = 12.1$ s^{-1}) is not slow enough to explain the low k_{cat} value of this substrate. Hence, another slow step, product release, must be partially rate-limiting. While PP_i release is probably rapid on the basis of the large $K_I^{intercept}$ (see above) (*17*), 8-oxo-dGMP release may well be slow since its K_D is 52 nM as determined by both isothermal titration calorimetry and by its K_I^{slope} (49 nM), indicating very tight binding of this product to the enzyme (*17*). $^1H-^{15}N$ HSQC titration of MutT with 8-oxo-dGMP showed that, unlike the case of dGMP, no stepwise changes in chemical shifts with each addition of 8-oxo-dGMP were observed. Instead, stepwise decreases in the *intensities* of 62 cross-peaks, together with the appearance of 62 new cross-peaks, occurred with each addition of 8-oxo-dGMP, indicating the tight binding and slow exchange of 8-oxo-dGMP between the free and enzyme-bound forms (*17*). This tight binding and slow exchange suggest that the release of the 8-oxo-dGMP product might well be rate-limiting in the MutT-catalyzed hydrolysis of 8-oxo-dGTP.

Accordingly, global fitting of the burst data to Scheme 1 yielded a value of 3.9 s^{-1} for k_4, the rate constant for 8-oxo-dGMP release, and a value of 160 s^{-1} for k_3, the rate constant for PP_i release (Table 1). A k_{cat} value of 2.6 s^{-1} was calculated with eq 5 from k_2, k_3, k_4, and k_5, in excellent agreement with the experimental k_{cat} of 2.8 s^{-1} from steady state measurements (*16*) (Table 2). Similarly, a k_{cat} of 2.7 s^{-1} was calculated with eq 6, which assumes fast dissociation (k_3) of PP_i, and a k_{cat} of 2.9 s^{-1} was calculated with an equation of the form of eq 8 containing only the partially rate-limiting k_4 and k_5 steps. However, a 31% larger k_{cat} of

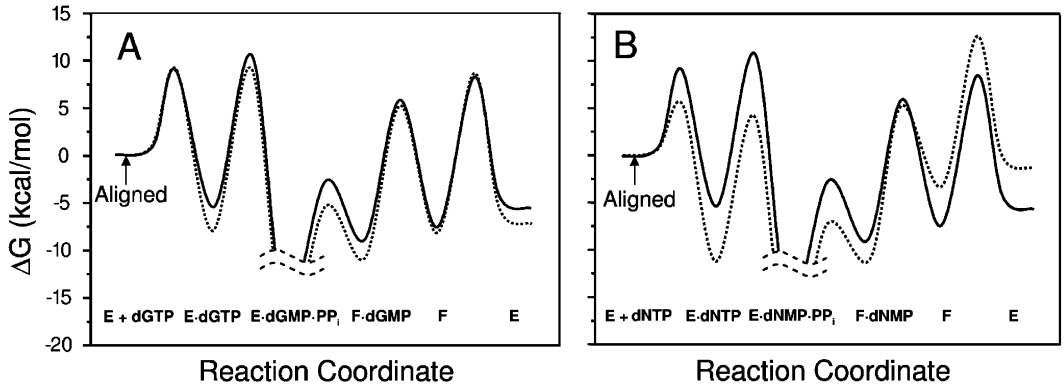

FIGURE 7: Free energy diagrams of the MutT reaction from transient kinetic data. (A) Comparison of the free energy diagrams for the Mg^{2+}-activated (—) and Mn^{2+}-activated (•••) hydrolysis of dGTP, catalyzed by MutT, aligned at the initial free energy level. The concentrations of substrates and products are adjusted to their respective in vivo levels: [dGTP] = 100 μM (*8*), [dGMP] = 9.1 μM (*33*), and [PP_i] = 500 μM (*34*). (B) Comparison of the free energy diagrams for the hydrolysis of 8-oxo-dGTP (•••) and dGTP (—), catalyzed by Mg^{2+}-activated MutT, aligned at the initial free energy level. To compare the two reactions under identical conditions, the concentrations of substrates and products are adjusted to the in vivo levels of dGTP, dGMP, and PP_i given in panel A. The barrier heights are from the individual rate constants in Table 1. In all cases, the free energy level of the E−dNMP−PP_i complex was undefined because the rate constant of the reverse of the hydrolytic step (k_{-2}) was too slow to be determined. The equilibrium constant (*K*) for the hydrolysis of free NTP and H_2O to yield NMP and PP_i equals 9.66×10^7 (*35*).

3.4 s^{-1} was calculated by assuming a fast iso step (k_5) with an equation of the form of eq 6, and a 3.2-fold larger k_{cat} of 7.8 s^{-1} was calculated with eq 7, which assumes fast dissociation (k_4) of 8-oxo-dGMP. These results are consistent with partially rate-limiting 8-oxo-dGMP release (k_4), partially rate-limiting enzyme isomerization (k_5), and a fast chemical step (k_2). Accordingly, a significant inhibitory effect on k_{cat} was found when the relative microviscosity was increased with sucrose (Figure 3), yielding a slope of 0.38 ± 0.04, consistent with partially rate-limiting 8-oxo-dGMP release. With Mg^{2+}-activated dGTP hydrolysis, in contrast, the slow steps are the chemical step (k_2) and the enzyme isomerization step (k_5) with only a small contribution of dGMP release (k_4) (Table 1).

CONCLUSIONS

To our knowledge, this study represents the first transient state kinetic analysis of the reaction pathway of a Nudix enzyme. The individual rate constants for each step in the MutT-catalyzed reaction, determined by global fitting of single- and multiple-turnover experiments (Table 1), confirm an iso kinetic mechanism (Scheme 1 and Figure 1) which was previously proposed on the basis of product inhibition studies alone (*17*). In this iso mechanism, the dissociation of products leaves an altered form of the enzyme (F), which slowly reverts, with a rate constant k_5, to the form that binds substrate (E).

Two sets of observations strongly support an iso kinetic mechanism. First, the substrates dGTP and 8-oxo-dGTP bind very slowly to MutT as measured by k_{on}^{app} values which are well below the diffusion limit in single-turnover experiments. Second, one or more rate-limiting step follows the chemical step as detected by bursts of product formation in multiple-turnover experiments. The major rate-limiting step following the chemical step was found to be the iso step. Nucleotide product release also contributed to rate limitation in the Mn^{2+}-activated hydrolysis of dGTP and in the Mg^{2+}-activated hydrolysis of 8-oxo-dGTP, as confirmed by viscosity effects on k_{cat}. The chemical step was also partially rate-limiting in all cases, although much less so with 8-oxo-dGTP. With the poor substrate dCTP, where the hydrolytic step is 36-fold slower than the iso step, no burst is detected, and chemistry is fully rate-limiting.

Changing the metal activator for dGTP hydrolysis from Mg^{2+} to the tighter-binding Mn^{2+} did not change the rate constant for substrate binding (k_1), consistent with the initial formation of a second-sphere complex, but decreased the rate constant (k_5) of the iso step 5.8-fold and its reverse (k_{-5}) 25-fold (Table 1), consistent with the iso step being a ligand substitution reaction on the enzyme-bound divalent cation (Figure 1). Figure 7A compares free energy diagrams for the Mg^{2+}- and Mn^{2+}-activated hydrolysis of dGTP catalyzed by MutT (*31*). With Mn^{2+} as the activator, tighter substrate binding (k_{-1}/k_1), slower release of dGMP (k_4), and a slower iso step (k_5) and its reverse (k_{-5}) are seen (Table 1).

Figure 7B compares the free energy diagrams for the MutT-catalyzed hydrolysis of 8-oxo-dGTP with that of dGTP (*31*) and shows that, with the exception of the iso step (k_5) and its reverse (k_{-5}), the rate constants of all other steps are different with the preferred substrate, 8-oxo-dGTP. The results (Table 1) also provide a detailed explanation of why 8-oxo-dGTP is a better substrate than dGTP at low substrate concentrations. First, the E-form of MutT binds 8-oxo-dGTP 395-fold faster than dGTP, with a second-order rate constant ($k_1 = 7.5 \times 10^8$ M^{-1} s^{-1}) closely approaching the diffusion limit. The faster binding of 8-oxo-dGTP may reflect the evolutionary adaptation of MutT to its optimal substrate. Second, 8-oxo-dGTP dissociates from the enzyme−substrate complex 46-fold slower than dGTP (Table 1). These two differences result in an overall 1.8×10^4-fold tighter binding of 8-oxo-dGTP than of dGTP to the active form of MutT. This tighter binding makes 8-oxo-dGTP a 395-fold better substrate than dGTP at low substrate concentrations, as measured by k_1, and 385-fold better as measured by k_{cat}/K_m. Hence, the MutT enzyme can hydrolyze 8-oxo-dGTP at very low substrate concentrations, as would be the case in vivo for this rare, oxidized, and mutagenic nucleotide. The estimated concentration of 8-oxo-dGTP in *E. coli* is ≤0.34 μM, while that of dGTP has been measured as 100 μM (*8*). Under these extreme conditions, it is estimated, from the

steady state k_{cat} and K_m values of these competing substrates (*32*), that the MutT-catalyzed hydrolysis of 8-oxo-dGTP would be 1.3-fold faster than the hydrolysis of dGTP. At the lower concentration of dGTP found in mammalian cells (5.2 μM) (*33*), 8-oxo-dGTP hydrolysis would be 24-fold faster than dGTP hydrolysis. The 3.0-fold faster hydrolytic step (k_2) with 8-oxo-dGTP than with dGTP (Table 1) ensures rapid catalytic turnover despite the partially rate-limiting release of the 8-oxo-dGMP product, and iso steps. Hence, the MutT enzyme has evolved to hydrolyze mutagenic nucleotides such as 8-oxo-dGTP more rapidly than dGTP at the low levels of these compounds that are present in cells.

ACKNOWLEDGMENT

We are grateful to Dr. Rachel Green and Dr. Jon R. Lorsch for making the rapid quench instrument available to us, to Ms. Julie L. Brunelle for helpful advice on rapid quench methodology, and to Dr. James T. Stivers, Dr. Philip A. Cole, Dr. W. W. Cleland, and Dr. Irwin A. Rose for valuable comments.

REFERENCES

1. Bessman, M. J., Frick, D. N., and O'Handley, S. F. (1996) The MutT proteins or "nudix" hydrolases, a family of versatile, widely distributed "housecleaning" enzymes, *J. Biol. Chem. 271*, 25059−25062.
2. Weber, D. J., Bhatnagar, S. K., Bullions, L. C., Bessman, M. J., and Mildvan, A. S. (1992) NMR and isotopic exchange studies of the site of bond cleavage in the MutT reaction, *J. Biol. Chem. 267*, 16939−16942.
3. Maki, H., and Sekiguchi, M. (1992) MutT protein specifically hydrolyzes a potent mutagenic substrate for DNA synthesis, *Nature 355*, 273−275.
4. Cheng, K. C., Cahill, D. S., Kasai, H., Nishimura, S., and Loeb, L. A. (1992) 8-Hydroxyguanine, an abundant form of oxidative DNA damage, causes G- - - -T and A- - - -C substitutions, *J. Biol. Chem. 267*, 166−172.
5. Treffers, H. P., Spinelli, V., and Belser, N. O. (1954) A factor (or mutator gene) influencing mutation rates in *Escherichia coli*, *Proc. Natl. Acad. Sci. U.S.A. 40*, 1064−1071.
6. Yanofsky, C., Cox, E. C., and Horn, V. (1966) The unusual mutagenic specificity of an *E. coli* mutator gene, *Proc. Natl. Acad. Sci. U.S.A. 55*, 274−281.
7. Tsuzuki, T., Egashira, A., Igarashi, H., Iwakuma, T., Nakatsuru, Y., Tominaga, Y., Kawate, H., Nakao, K., Nakamura, K., Ide, F., Kura, S., Nakabeppu, Y., Katsuki, M., Ishikawa, T., and Sekiguchi, M. (2001) Spontaneous tumorigenesis in mice defective in the MTH1 gene encoding 8-oxo-dGTPase, *Proc. Natl. Acad. Sci. U.S.A. 98*, 11456−11461.
8. Tassotto, M. L., and Mathews, C. K. (2002) Assessing the metabolic function of the MutT 8-oxo-dGTPase in *Escherichia coli* by nucleotide pool analysis, *J. Biol. Chem. 277*, 15807−15812.
9. Mildvan, A. S., Weber, D. J., and Abeygunawardana, C. (1999) Solution structure and mechanism of the MutT pyrophosphohydrolase, *Adv. Enzymol. Relat. Areas Mol. Biol. 73*, 183−207.
10. Mildvan, A. S., Xia, Z., Azurmendi, H. F., Saraswat, V., Legler, P. M., Massiah, M. A., Gabelli, S. B., Bianchet, M. A., Kang, L.-W., and Amzel, L. M. (2005) Structures and mechanisms of Nudix hydrolases, *Arch. Biochem. Biophys. 433*, 129−143.
11. Abeygunawardana, C., Weber, D. J., Gittis, A. G., Frick, D. N., Lin, J., Miller, A.-F., Bessman, M. J., and Mildvan, A. S. (1995) Solution structure of the MutT enzyme, a nucleoside triphosphate pyrophosphohydrolase, *Biochemistry 34*, 14997−15005.
12. Lin, J., Abeygunawardana, C., Frick, D. N., Bessman, M. J., and Mildvan, A. S. (1997) Solution structure of the quaternary MutT-M^{2+}-AMPCPP-M^{2+} complex and mechanism of its pyrophosphohydrolase action, *Biochemistry 36*, 1199−1211.
13. Massiah, M. A., Saraswat, V., Azurmendi, H. F., and Mildvan, A. S. (2003) NMR and mutagenesis studies of the structure of the MutT-Mg^{2+}-8-oxo-dGMP complex, *Biochemistry 42*, 10140−10154.
14. Frick, D. N., Weber, D. J., Gillespie, J. R., Bessman, M. J., and Mildvan, A. S. (1994) Dual divalent cation requirement of the MutT dGTPase, *J. Biol. Chem. 269*, 1794−1803.
15. Harris, T. K., Wu, G., Massiah, M. A., and Mildvan, A. S. (2000) Mutational, kinetic, and NMR studies of the roles of conserved glutamate residues and of Lys-39 in the mechanism of the MutT pyrophosphohydrolase, *Biochemistry 39*, 1655−1674.
16. Saraswat, V., Azurmendi, H. F., and Mildvan, A. S. (2004) Mutational, NMR, and NH exchange studies of the tight and selective binding of 8-oxo-dGMP by the MutT pyrophosphohydrolase, *Biochemistry 43*, 3404−3414.
17. Saraswat, V., Massiah, M. A., Lopez, G., Amzel, L. M., and Mildvan, A. S. (2002) Interactions of the products 8-oxo-dGMP, dGMP, and pyrophosphate with the MutT nucleoside triphosphate pyrophosphohydrolase, *Biochemistry 41*, 15566−15577.
18. Rebholz, K. L., and Northrop, D. B. (1995) Kinetics of iso mechanisms, *Methods Enzymol. 249*, 211−240.
19. Cleland, W. W. (1977) Determining the chemical mechanisms of enzyme catalyzed reactions by kinetic studies, *Adv. Enzymol. 45*, 273−387.
20. Rose, I. A. (1998) How fumarase recycles after the malate → fumarate reaction. Insights into the reaction mechanism, *Biochemistry 37*, 17651−17658.
21. Rose, I. A. (1997) Restructuring the active site of fumarase for the fumarate to malate reaction, *Biochemistry 36*, 12346−12354.
22. Johnson, K. A. (1992) Transient-state kinetic analysis of enzyme reaction pathways, *Methods Enzymol. 134*, 677−705.
23. Abeygunawardana, C., Weber, D. J., Frick, D. N., Bessman, M. J., and Mildvan, A. S. (1993) Sequence specific assignments of the backbone ^1H, ^{13}C, and ^{15}N resonances of the MutT enzyme by heteronuclear multidimensional NMR, *Biochemistry 32*, 13071−13080.
24. Mo, J.-Y., Maki, H., and Sekiguchi, M. (1992) Hydrolytic elimination of a mutagenic nucleotide, 8-oxo-dGTP, by human 18-kilodalton protein: Sanitization of nucleotide pool, *Proc. Natl. Acad. Sci. U.S.A. 89*, 11021−11025.
25. Kasai, H., and Nishimura, S. (1984) Hydroxylation of deoxyguanosine at the C-8 position by ascorbic acid and other reducing agents, *Nucleic Acids Res. 12*, 2137−2145.
26. Trilink Biotechnologies, Inc. (1999) *Product Data Sheet*, San Diego.
27. Zhang, H., Wood, O. L., Papermaster, S. F., Nielsen, C. J., and Ussery, M. A. (1997) Palindromic oligonucleotide-directed enzymatic determination of 2′-deoxythymidine 5′-triphosphate and 2′-deoxycytidine 5′-triphosphate in human cells, *Anal. Biochem. 252*, 143−152.
28. Kuzmic, P. (1996) Program DynaFit for the Analysis of Enzyme Kinetic Data: Application to HIV Proteinase, *Anal. Biochem. 237*, 260−273.
29. Cole, P. A., Burn, P., Takacs, B., and Walsh, C. T. (1994) Evaluation of the catalytic mechanism of recombinant human Csk (C-terminal Src kinase) using nucleotide analogs and viscosity effects, *J. Biol. Chem. 269*, 30880−30887.
30. *CRC Handbook of Chemistry and Physics*, 58th ed. (1978) p D-261, CRC Press Inc., Cleveland, OH.
31. Cleland, W. W., and Northrop, D. B. (1999) Energetics of substrate binding, catalysis, and product release, *Methods Enzymol. 308*, 3−27.
32. Segal, I. H. (1975) *Enzyme Kinetics*, pp 113−114, John Wiley and Sons, New York.
33. Traut, T. W. (1994) Physiological concentrations of purines and pyrimidines, *Mol. Cell. Biochem. 140*, 1−22.
34. Kukko-Kalske, E., Lintunen, M., Inen, M. K., Lahti, R., and Heinonen, J. (1989) Intracellular PP_i concentration is not directly dependent on amount of inorganic pyrophosphatase in *Escherichia coli* K-12 cells, *J. Bacteriol. 171*, 4498−4500.
35. Frey, P. A., and Arabshahi, A. (1995) Standard free energy change for the hydrolysis of the α,β-phosphoanhydride bridge in ATP, *Biochemistry 34*, 11307−11310.

BI0513599